Earthquake Geotechnical Engineering for Protection and Development of Environment and Constructions – Silvestri & Moraci (Eds)
© 2019 Associazione Geotecnica Italiana, Rome, Italy, ISBN 978-0-367-14328-2

Seismic performance of geosynthetic-reinforced retaining walls: Experimental tests vs numerical predictions

G. Di Filippo & G. Biondi
Department of Engineering, University of Messina, Italy

N. Moraci
Department of Civil, Environmental, Energy and Material Engineering, Mediterranea University, Reggio Calabria, Italy

ABSTRACT: In seismic areas geosynthetic-reinforced soil walls (*GRSWs*) represent a suitable alternative to conventional concrete retaining structures. Despite pseudo-static procedures still represent the basis for seismic design, the need of shifting to displacement-based analyses is widely recognized. In this framework, the paper presents a modified sliding block model proposed for the evaluation of the seismic performance of *GRSWs*. The model accounts for the soil-reinforcements interaction under cyclic loading conditions and for the compliance of the earth-reinforced zone which, in turn, depend on the stiffness of both reinforced soil and reinforcements. The model capability has been checked through a comparison between numerical predictions and dynamic centrifuge test results. The comparison is presented and discussed in terms of time-histories and final permanent values of seismic-induced displacements.

1 INTRODUCTION

Most of recent post-seismic surveys revealed that earth-reinforced retaining structures have suffered minor or negligible damages in comparison with conventional concrete retaining walls. Thus, these structures are nowadays considered a suitable alternative especially in high seismicity areas.

As for other geotechnical systems, such as natural slopes and concrete retaining walls (e.g. Narasimha Reddy *et al*., 2008; Huang & Lou, 2010, Biondi *et al*., 2011, 2014), pseudo-static procedures still represent the basis for seismic design of earth-reinforced retaining structures. Indeed, even if post-seismic serviceability conditions are better related to permanent deformations rather than to stresses, the latter can be predicted more accurately, and this helped support the continuing use of stress-based prediction of the seismic performance of geotechnical systems. The shifting from force-balance approaches to displacement-based analyses implies recognizing that retaining structures can experience permanent deformations and displacements which must be predicted to check the possible occurrence of a limit state. Accordingly, design procedures can be based on the comparison between the expected earthquake-induced permanent displacements and suitably selected allowable threshold values.

This paper focus on the evaluation of seismic performance of geosynthetic-reinforced soil walls (*GRSWs*) and describe the main features of a simplified numerical model aimed to estimate the earthquake-induced permanent displacements through a modified Newmark-type approach. The model allow accounting for the possibly occurring coupling between the fundamental frequencies of the *GRSW* and the frequency content of the input motion and it is able to describe the isolation effect due to the soil-geosynthetic interfaces which can significantly reduce the input acceleration pulses in the wall leading to a satisfactorily seismic performance. The capability of the model has been checked comparing experimental data obtained in

dynamic centrifuge tests and numerical predictions. The comparison results are presented and discussed in the paper.

2 ON THE ANALYSIS OF SEISMIC PERFORMANCE OF GRSWs

As an alternative to finite-difference or finite-element dynamic numerical analyses, earthquake-induced permanent displacements of *GRSWs* may be predicted through simplified model derived from the original Newmark sliding-block approach introducing the effects of the soil-reinforcements interaction and of the compliance of the earth-reinforced zone. The latter issue allows splitting the available approaches into two main categories.

A first category includes those studies in which, as in the conventional Newmark's sliding block approach: *i*) the reinforced soil mass involved in a potential failure mechanism is treated as a rigid-plastic block; *ii*) permanent displacements start when the earthquake-induced acceleration overcome the corresponding yield acceleration $a_c = k_c \cdot g$; *iii*) permanent displacements are triggered by unbalanced forces, cumulate when the relative velocity is positive and are computed integrating twice the equation of motion of a rigid body. In these procedures the equation of motion differs from that of a rigid block sliding on a horizontal plane only for a displacement coefficient C which summarizes the geometrical and mechanical properties of the *GRSW* and the main features of the failure mechanism. Several authors proposed solutions and procedures to estimate k_c and C and to select a suitable value of the pseudo-static seismic coefficient which leads to an equivalence between the pseudo-static and the displacement-based analysis (e.g. Cai & Bathurst 1996; Ausilio *et al*. 2000; Gaudio *et al.*, 2018).

Few approaches were developed to account for the compliance of the reinforced soil mass and consist in simplified dynamic analyses mainly aimed to predict the occurrence of ground motion amplification and the magnitude of earthquake-induced permanent displacements. The extent to which the dynamic response computed accounting for system compliance, deviates from that computed according to the rigid block hypothesis, depends on the possible coupling between the frequency content of the input motion and the fundamental frequencies of vibration of *GRSWs*; the frequencies, in turn, depend on the mechanical properties of both soil and reinforcements and on the geometry of the reinforced zone. *GRSWs* generally consist of stiff dense compacted granular soils but they could extend to extreme heights (leading to very flexible structures) and the contacts between soil and geosynthetics could represent soft interfaces. Accordingly, it could be expected that input ground motions can vary significantly, both in amplitude and phase, along the depth of the reinforced zone and the resultant driving force acting on the potential failure mass will not be proportional to the acceleration as in the case of a conventional Newmark-type analysis. In this context, Carotti & Rimoldi (1998) proposed a multi-degree of freedom lumped mass non-linear model and used the modal decoupling technique for the evaluation of dynamic response. In the model, the soil masses of each layer behave as a visco-elastic material and the behaviour of soil-geosynthetic interfaces were described through specific interlayer dynamic interactions calibrated using the experimental results of the cyclic tensile tests carried out by Montanelli & Moraci (1997).

Paulsen & Kramer (2004) presented a 2-degree of freedom model able to reproduce the primary mechanisms that contribute to the occurrence of earthquake-induced permanent deformations in *GRSWs* with approximately 1H:2V face (about 60°), height up to 8 m and length of reinforcements ranging from 0.25 to 1 time the slope height. Kramer & Paulsen (2004) carried out a parametric analysis to show the relationships between the magnitude of earthquake-induced permanent displacements of *GRSWs* and several parameters affecting their seismic response.

3 PROPOSED NUMERICAL MODEL

The proposed numerical model refers to a *GRSW* of height H, with a face inclination θ and N layers of equally-spaced (s) geosynthetic reinforcements of length L (Figure 1a): γ, φ and v_s

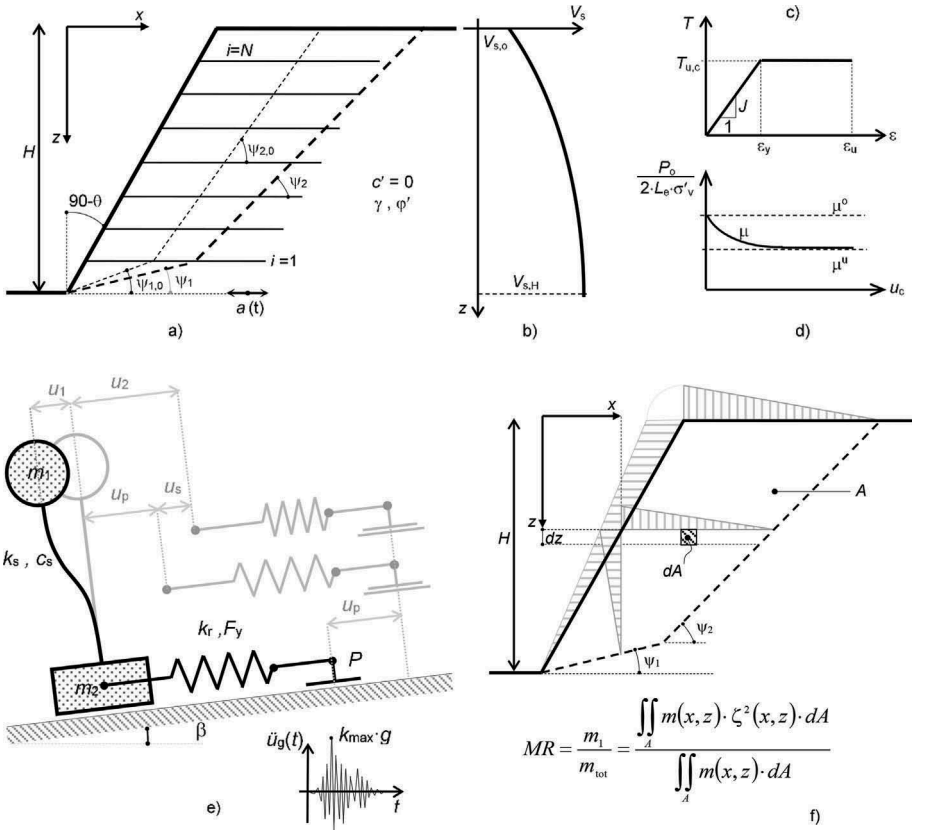

$$MR = \frac{m_1}{m_{tot}} = \frac{\iint_A m(x,z)\cdot \zeta^2(x,z)\cdot dA}{\iint_A m(x,z)\cdot dA}$$

Figure 1. a-d) Reference scheme; e) rheological model; f) scheme to define the shape function.

are the unit weight, the angle of shear strength and an average value of the shear wave velocity of the backfill soil (whose profile is described in Figure 1b), respectively; J and, T_u represent the '*in air*' wide-width stiffness and the tensile strength of the reinforcements (Figure 1c); δ_i is the friction angle schematizing the shear strength available along the i^{th} soil-geosynthetic interface. The input motion consists of a horizontal acceleration time-history $a(t)$, representing the motion at the base of the *GRSW*, with peak value $a_{max} = k_{max} \cdot g$.

As in the study by Paulsen & Kramer (2004) the actual *GRSW* was condensed into a simple rheological model consisting in the 2-degree of freedom (*2DOF*) system shown in Figure 1e: two masses, m_1 and m_2, define a compliant two-block system schematizing the portion of the actual *GRSW* involved in the failure mechanism, which has distributed total mass $m = m_1 + m_2$, distributed elasticity and infinite number of degrees of freedom; three discrete elements, the compliant two-block system, an elasto-plastic spring and a Coulomb slider, allow reproducing the primary mechanism that characterizes the dynamic response of *GRSWs: i*) possible amplification of ground motion due to coupling between system and input frequencies; *ii*) possible occurrence of permanent deformations due to soil shearing, to stretching and potential yielding of reinforcements and, finally, to the possibly occurring pull-out of reinforcements.

Differently from the model by Paulsen & Kramer (2004), the effect of the reinforcement ductility $\chi = \varepsilon_u/\varepsilon_y$ (Figure 1c) can be accounted for in the displacement analysis and proper values of the '*in air*' wide-width stiffness are used according to the experimental results by Cardile *et al.* (2016, 2017). Also, the influence of the static effective stress state and of the soil-geosynthetic interaction under cyclic loading conditions (Moraci *et al.* 2017) is considered for a proper estimate of the current value of the interface apparent friction coefficient μ (Figure 1c). Specifically, suitable values of δ_i can be adopted for each layer of geosynthetic

reinforcements and the special case $\delta_i = \delta = \varphi$ lead to the assumption adopted by Paulsen & Kramer (2004). Finally, a proper evaluation of the soil mass involved in the seismic failure mechanism and of the shape function that approximates the fundamental vibration mode of the GRSW, are also introduced.

All the main features of the proposed model are described in the papers by Biondi & Moraci (2014) and Di Filippo *et al.* (2014). Herein, only some peculiarities of the proposed model are presented and discusses. Specifically, the attention is focused on the procedures adopted to evaluate the mass ratio $MR = m_1/m$ (which controls the value of the masses defining the *2DOF* system) and to define a proper shape function which allow approximate the actual dynamic response of the *GRSW* using the theory of generalized SDOF systems.

3.1 *Soil mass involved in the failure mechanism*

The evaluation of the soil mass involved in the failure mechanism is a crucial aspect in order to fit the actual behavior of both soil and reinforcements and to reliably reproduce the effects of their interaction. Herein m and m_o denote the total masses corresponding to a bi-linear seismic (m) or static (m_o) failure surface whose geometry is defined by the angles ψ_1 and ψ_2 or $\psi_{1,o}$ and $\psi_{2,o}$ described in Figure 1a. Simple geometric considerations lead to the following non-dimensional expression of the soil mass m involved in the potential seismic failure mechanism:

$$\frac{m \cdot g}{0.5 \cdot \gamma \cdot H^2} = \cot\psi_1 \cdot \left(2 \cdot \frac{s}{H} - \frac{s^2}{H^2}\right) - \cot\psi_2 \cdot \left(2 \cdot \frac{s}{H} - \frac{s^2}{H^2} - 1\right) - \cot\theta \tag{1}$$

If ψ_1 and ψ_2 are replaced by $\psi_{1,o}$ and $\psi_{2,o}$ in eq.(1), the mass m_o can be computed.

As in Paulsen & Kramer (2004) the shape of the seismic failure surface is evaluated starting from the shape of a static failure surface describing the flattening through appropriate functions of the peak horizontal acceleration of the input motion k_{max}, of the angle of shear resistance φ, of the reinforcement spacing (s), length (L) and mechanical properties (J, T_u) and, finally, of the soil-geosynthetic interface friction angle. Through a best-fit procedure, based on least squares method, the static log-spiral failure surfaces deteced by Ling *et al.* (1997) were reproduced using a 4th order polynomial interpolation and the following bi-linear approximation:

$$\begin{aligned} \tan\psi_{1,o} &= \frac{\frac{s}{H}}{A_4 \cdot \left(\frac{s}{H}\right)^4 + A_3 \cdot \left(\frac{s}{H}\right)^3 + A_2 \cdot \left(\frac{s}{H}\right)^2 + A_1 \cdot \left(\frac{s}{H}\right)} \\ \tan\psi_{2,o} &= \frac{1 - \frac{s}{H}}{A_4 \cdot \left[1 - \left(\frac{s}{H}\right)^4\right] + A_3 \cdot \left[1 - \left(\frac{s}{H}\right)^3\right] + A_2 \cdot \left[1 - \left(\frac{s}{H}\right)^2\right] + A_1 \cdot \left[1 - \left(\frac{s}{H}\right)\right]} \end{aligned} \tag{2}$$

being $A_1, \ldots, A_4$ regression coefficients whose best estimates are given in Figure 2a for $\theta = 60°$.

3.1 *Shape function*

The masses m_1 and m_2 (Figure 1b) define a compliant two-block system schematizing the actual *GRSW* having a distributed total mass m, distributed elasticity and infinite number of degrees of freedom. According to the theory of *generalized SDOF systems*, by restricting the wall deformations to a single shape function that approximates the fundamental vibration mode, it is possible to obtain an approximation of its actual dynamic response that is sufficiently accurate for practical purposes. In essence, by assuming that the actual continuous compliant system deforms in a specific pattern, its dynamic response coincides to that of generalized *SDOF* system with natural frequency and generalized mass equal to those of the continuous system. The generalized mass represents the portion *MR* of the total mass m that responds dynamically. Paulsen & Kramer (2004) assimilated it to the upper mass $m_1 = MR \cdot m$, and for a typical $\theta = 60°$ *GRSW*, assumed $MR = 0.14$.

Due to the previously described differences in the evaluation of $\psi_{1,o}$ and $\psi_{2,o}$, Di Filippo *et al.* (2014) derived the equations relevant to the evaluation of *MR* as a function of the angles

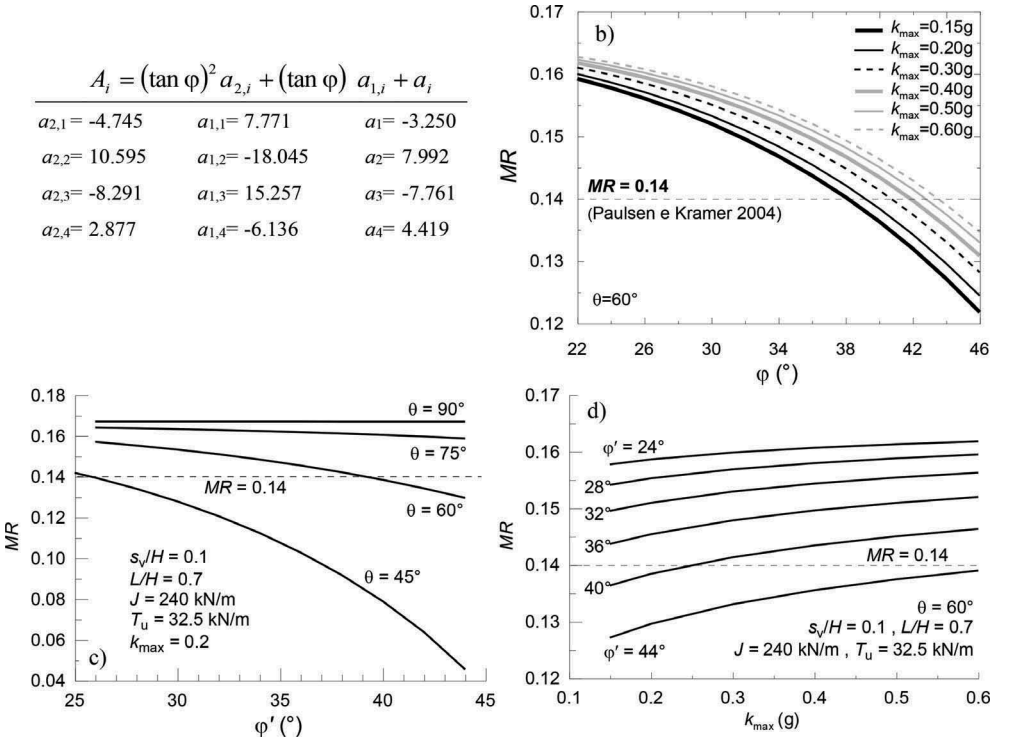

Figure 2. a) Regression coefficients for the polynomial interpolation of static failure surfaces by Ling et al. 1997 (θ = 60°); b) Values of the mass ratio *MR* computed for θ = 60° and different values of k_{max} and φ; c-d) Influence of k_{max} and φ on the computed values of the mass ratio.

ψ_1 and ψ_2 which, in turn, depend on all the parameters affecting the geometry of the seismic failure surface: θ, k_{max}, φ, *s, L, δ, j* and T_u.

These equations were derived using the shape function described in Figure 1d which assumes that the material above the seismic failure surface move horizontally with maximum displacement at the crest of the wall, zero displacements for points along the failure surface and linearly varying displacements of all the points between the wall face and the failure surface. According to Di Filippo *et al.* (2014), the mass ratio *MR* is mostly affected by the parameters θ, k_{max} and φ. In Figure 2b the values of *MR* computed for the case θ = 60°, *s*/*L* = 0.1, *L*/*H* = 0.7, *J* = 240 kN/m and T_u = 32.5 kN/m are plotted versus φ for values of k_{max} in the range 0.15 ÷ 0.60 *g*; δ_i = δ = φ was assumed to compare the results with those by Paulsen & Kramer (2004). For φ in the range 20°÷60°, which covers the whole range of values relevant for both cohesive and granular materials, *MR* is in the range 0.10-0.16 with the higher values corresponding to the lower angle of shear strength and to the lower peak horizontal acceleration k_{max}. For φ ≥ 38°, as it is usual for *GRSW* realized using granular dense materials, the value *MR* = 0.14 assumed by Paulsen & Kramer (2004) for θ = 60° can be considered as a suitable upper bound, regardless the values of k_{max}. The relevant influence of θ, φ and k_{max} is shown in the Figures 2c and 2d, where the values of the other model parameters are also specified.

4 NUMERICAL PREDICTIONS VS EXPERIMENTAL MEASUREMENTS

The comparison between experimental measurements and numerical predictions represent the proper instrument to check the capability of predictive models. Concerning the seismic performance of both un-reinforced and reinforced soil slopes and earth-retaining structures, this

comparison is generally carried out in terms of yield acceleration coefficient, time-histories of cumulated permanent displacements and final permanent displacements (e.g. Watanabe *et al*., 2003; Huang *et al*., 2011; Bandini *et al.*, 2015; Biondi *et al*. 2016; Capilleri *et al*. 2018, 2019).

Herein, the capability of the proposed numerical model was checked against the results of the 30g dynamic centrifuge tests carried out by Andersen (1997) on 8 physical models (namely Test *A1*, …, *A8*) of a prototype GRSW of height $H = 6.1$ m with a face inclination $\theta = 60$ °, realized using Unimin 4060 sand and lightweight nonwoven geotextiles (7 tests) or geogrid (1 test). In the model L/H is in the range $0.1875 \div 0.375$ and the reinforcement spacing vary from 0.61 m 0.41 m. Table 1 summarizes the main properties of the tested physical models. A sinusoidal waveform has been applied to each model with constant frequency equal to 2 Hz, a prototype amplitude equal to 0.5 g and a number of cycles equal to 5.

During the tests, horizontal displacements at the top, middle and bottom of the wall face were monitored, and the deformed shape of the models were detected at the end of the shakings.

The numerical simulations of these experimental tests were carried out into two phases: the first involved the determination of the model parameters starting from the geometrical and mechanical properties of the physical models; the second concern with the numerical integration of the equations of motion of the *2DOF*.

Herein, the comparison between measured and predicted displacements is carried out comparing the permanent displacements of the lower mass (m_2) of the numerical model with the displacement measured at the top of the face of the physical models. The comparison results are presented in Figures 3 and 4 in terms final values of cumulated permanent displacement (Figure 3) and displacement time-histories (Figure 4).

As it can be observed from the time-histories plotted in Figure 4, whatever are the reinforcements length (tests *A1, A2* and *A3*), spacing (tests *A6* and *A7*) and stiffness (tests *A5, A8*), the proposed numerical model allows predicting with sufficient accuracy the time instant at which permanent displacements start to develop and the overall displacement time-history.

Table 1. Geometrical and mechanical parameters of the prototype models tested by Andersen (1997).

ID	L (m)	s (m)	J (kN/m)	T_u (kN/m)	L/H	s/L
A1	1.52	0.61	40.80	4.36	0,249	0,401
A2	1.14	0.61	40.80	4.36	0,187	0,535
A3	1.91	0.61	40.80	4.36	0,313	0,319
A4	1.52	0.61	7.78	1.37	0,249	0,401
A5	2.29	0.61	7.78	1.37	0,375	0,266
A6	1.52	0.41	7.78	1.37	0,249	0,270
A7	1.52	0.51	7.78	1.37	0,249	0,336
A8	2.29	0.61	32.83	22.06	0,375	0,266

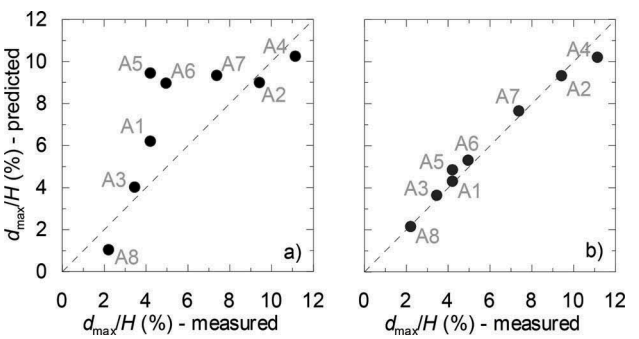

Figure 3. – Final value of permanent displacements: comparison between experimental measurements (Andersen, 1997) and numerical predictions obtained by Paulsen & Kramer 2004 (a) and in the present work (b).

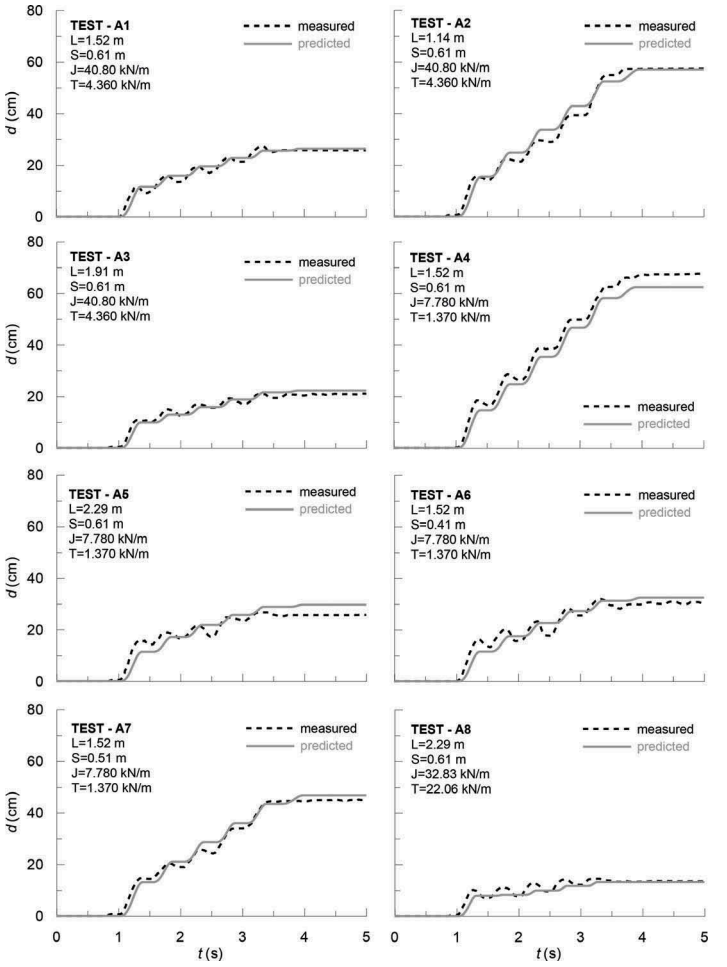

Figure 4. – Displacement time-histories: comparison between experimental measurements (Andersen, 1997) and numerical predictions obtained by Paulsen & Kramer 2004 (a) and in the present work (b).

The computed values of final permanent displacements are also in a fair agreement with the measured values (Figure 4b), with relative errors generally lower that 10%, and an improvement of the predictive capability can be also observed in comparison with the predictions obtained by Paulsen & Kramer 2004 (Figure 4a).

5 CONCLUDING REMARKS

The paper describes the validation of a simplified model through the comparison between numerical predictions and the results of dynamic centrifuge tests carried out on prototype geosynthetic-reinforced soil walls of height $H = 6.1$ m and a face inclination $\theta = 60°$. Some of the main features of the model are presented and discussed focusing on the procedures adopted to approximate the actual dynamic response of the *GRSW*. The comparison results point out that whatever are the reinforcements length, spacing and stiffness, the proposed model allows predicting, with sufficient accuracy, the time instant at which displacements start to develop, the overall displacement time-history and the final value of cumulated permanent displacements.

ACKNOWLEDGEMENT

The research activity was carried out in the framework of the Research Project PON01_01869 (PON Ricerca e Competitività 2007-2013) titled "*Tecnologie e Materiali Innovativi per la Difesa del Territorio e la Tutela dell'Ambiente [TEMADITUTELA]*" and was funded by the European Union and by the Italian "*Ministero dell'Istruzione, della Ricerca e dell'Università*" e "*Ministero dello sviluppo sostenibile*".

REFERENCES

Andersen E., 1997. A centrifuge modeling study of the seismic response of geosynthetic-reinforced slopes. *MS thesis*, University of Washington, 148 pp.

Ausilio E., Conte E., Dente G., 2000. Seismic stability analysis of reinforced slopes. *Soil Dynamics and Earthquake Engineering, Elsevier*, 19 (2): 159–172.

Biondi G. Cascone E Rampello G. 2011. Valutazione del comportamento dei pendii in condizioni sismiche. *Rivista Italiana di Geotecnica*, 2011.

Biondi G, Cascone E, Maugeri M. 2014. Displacement versus pseudo-static evaluation of the seismic performance of sliding retaining walls. *Bulletin of Earthquake Engineering*, 2014, 12(3): 1239–1267.

Biondi G. & Moraci N., 2014. Opere di sostegno in terra rinforzata soggette ad azione sismica: recenti esperienze e previsioni del comportamento. *XXV Convegno Nazionale di Geotecnica*, Baveno 4–6 June, (in Italian).

Biondi G., Capilleri P, Motta E. (2016). Seismic displacements of retaining walls: Shaking table test results vs numerical predictions. *1st IMEKO TC4 Int. Workshop on Metrology for Geotechnics, Metro-Geotechnics* 2016.

Cai Z., Bathurst R.J., 1996. Seismic-induced permanent displacement of geosynthetic reinforced segmental retaining walls. *Canadian Geotechnical Journal*, 33: 937–955.

Capilleri P.P., Motta E., Biondi G. (2019). Comparison between shaking table test results and numerical predictions of seismic performance of a soil-wall system. *This Conference*.

Capilleri, P.P., Ferraiolo, F., Motta, E., Scotto, M. & Todaro, M. 2018. Static and Dynamic Analysis of two Mechanically Stabilized Earth Walls. *Geosynthetics International*.

Cardile, G., Moraci, N., Pisano, M., 2016. In-air Tensile Load-strain Behaviour of HDPE Geogrids Under Cyclic Loading. *Procedia Engineering* 158, 266–271.

Cardile, G., Moraci, N., Pisano, M., 2017. Tensile behaviour of an HDPE geogrid under cyclic loading: experimental results and empirical modelling. *Geosynthetics International* 24, 95–112.

Carotti A., Rimoldi P., 1998. A Nonlinear Model for the Seismic Response Analysis of Geosynthetic-Reinforced Soil Structures. *Geosynthetics International*, 5 (1-2): 167–201.

Di Filippo G., Biondi G., Moraci N., 2014. Analisi dinamica semplificata della risposta sismica di opere di sostegno in terra rinforzata. *XXV Convegno Nazionale di Geotecnica*, Baveno 4–6 June (in Italian).

Gaudio D., Masin, L., & Rampello S. (2018). A performance-based approach to design reinforced-earth retaining walls. *Geotextiles and Geomembranes*, 46(4): 470–485.

Huang C.C, Lou W.M. (2010). Behaviour of cantilever and geosynthetic-reinforced walls on deformable foundation. Geotextiles and Geomembranes, 28:5, 448–459.

Huang C.C., Horng J.C., Chang W.J., Chiou J.S., Chen C.H., 2011. Dynamic behaviour of reinforced walls e horizontal displacement response. *Geotextiles and Geomembranes* 29(3): 257–267

Kramer, S. L., Paulsen, S. (2004) - Seismic performance evaluation of reinforced slopes. *Geosynthetics International*, 11 (6): 429–438.

Ling, H. I., Leshchinsky, D., Perry, E. B. (1997). Seismic design and performance of geosynthetic-reinforced soil structure. *Geotechnique*, 48 (3), pp.347–373.

Montanelli F., Moraci N., 1997. Behaviour of Geogrids Under Cyclic Loads. *Geosynthetics' 97*, IFAI, Long Beach, California, USA, Vol. 2: 961–976

Moraci, N., Cardile, G., Pisano, M., 2017. Soil-geosynthetic interface behaviour in the anchorage zone. *Rivista italiana di geotecnica* 51, 5–25 (in Italian)

Narasimha Reddy G.V., Madhav M.R., Saibaba Reddy E. (2008). Pseudo-static seismic analysis of reinforced soil wall—Effect of oblique displacement. *Geotextiles and Geomembranes* 26 (2008) 393–403.

Paulsen S.B., Kramer S.L., 2004. A predictive model for seismic displacements of reinforced slopes. *Geosynthetics International*, 11(6): 407–428

Watanabe K., Munaf. Y., Koseki J., Tateyama M., Kojima K., 2003. Behaviours of several type of models retaining walls subjected to irregular excitation. *Soils and Foundations*, Vol. 43(5): 13–27.